



Steel Innovations Conference 2015
Auckland, New Zealand
3-4 September 2015

ANALYTICAL STUDY OF SEISMIC BEHAVIOUR OF COMPOSITE SLABS

F. Luo¹, A. Gholamhoseini² and G. A. MacRae³

ABSTRACT

This paper presents the results of finite element analysis on the seismic performance of composite slabs with a specific type of steel decking and slab geometry. Four different slab thicknesses were considered and their capacity to carry inertia-induced and in-plane transfer forces was studied. The effects of different arrangements, support conditions and presence of steel rebars in the slabs were investigated and discussed. It was shown that for the slab model selected, the effects of in-plane forces on out-of-plane deformations were negligible; steel reinforcing increased the slab strength by 82% when the applied load was perpendicular to steel decking ribs, but only 11% when the applied load was parallel to the ribs; and for slab thicknesses less than 135 mm failure occurred under the applied loads.

Introduction

Composite slabs consisting of profiled steel decking and structural concrete are increasingly used in buildings worldwide. In this system, the steel decking is normally continuous over two-spans between the supporting steel beams and during construction the concrete is poured to form a continuous one-way composite slab. The composite action between the steel decking and the hardened concrete is dependent on the transmission of horizontal shear stresses acting on the interface between the concrete slab and the steel decking.

In addition to carry the gravity loads, composite slabs act as a diaphragm to distribute the lateral (wind and earthquake) forces to the vertical elements of the lateral load resisting systems (such as frames and structural walls). Design engineers often assume composite slabs as fully rigid diaphragms without explicitly checking the load paths through diaphragms and the interaction of load-resisting structural elements such as concrete slab, steel decking, supporting beams and walls, etc. This is essentially due to the fact that there are few research studies and guidance available in open literature and design codes to show how these complexities can be considered and the assumptions be verified.

Many building failures in the past earthquakes have been reported of lack of composite slabs strength and poor detailing to transfer the earthquake-induced loads (Chaudhari et al. 2014). Transmission of transfer forces between different load-resisting elements in a building is an example of an important issue that is normally neglected in diaphragm design. It shall be highlighted that the value of transfer forces is often much greater than inertia-induced forces due to applied gravity loads and slabs self-weight.

Current design codes do not present a procedure to evaluate the seismic behaviour and strength of composite concrete slabs and if needed, this is often assessed by full scale tests. Designers often consider

¹Undergraduate Student, Dept. of Civil and Natural Resources Engineering, University of Canterbury, Christchurch 8140, New Zealand

²Postdoctoral Research Fellow, Dept. of Civil and Natural Resources Engineering, University of Canterbury, Christchurch 8140, New Zealand (email: alireza.gholamhoseini@canterbury.ac.nz)

³Associate Professor, Dept. of Civil and Natural Resources Engineering, University of Canterbury, Christchurch 8140, New Zealand

the composite floors as rigid and strong diaphragms for all seismic cases but this may not be necessarily correct and needs to be quantified. If the thickness of a composite slab is less than the minimum required, it will not be able to provide sufficient strength and stiffness and its performance in a severe earthquake to act as a rigid floor is quite questionable. It is emphasised here that since the thickness of the cross-section of a composite slabs is not constant due to the shape of steel decking, only part of concrete slab above decking trough is able to carry in-plane forces. As a result, sometimes the thickness of concrete above trough in a composite slab is considered as a key parameter in its seismic behaviour and strength. In many cases this thickness (above the trough of steel decking) is considered to be more than 50 mm but this shall be quantified for a specific combination of earthquake motion, steel decking type and thickness and concrete strength.



Figure 1. Composite slab in a steel frame structure.

As can be seen from the discussion above, there exists an urgent need to quantify the seismic behaviour and capacity of composite slabs with different slab thicknesses subjected to design inertia accelerations and transferred forces.

In order to address this need, answers are sought to the following questions in this paper:

- How do in-plane forces change out-of-plane deformations of composite slab caused by gravity loads?
- How does the presence of steel rebar affect the in-plane strength of a composite slab when carrying transfer forces?
- What is the difference in strength of a composite slab in different directions?
- What criteria should be used to determine the minimum thickness of a composite slab, and what should that thickness be?

Numerical Study

The good agreement between the finite element modelling and the test results obtained in many other studies suggests that far less expensive numerical modelling can be used to verify the seismic performance of composite slabs. Before performing any experimental study and in lieu of the expense and complexities involved with full-scale testing, a finite element analysis is usually proposed to simulate the slab performance.

The general purpose non-linear finite element software Abaqus (2011) was used in the present study to investigate the ultimate strength and seismic performance of composite slabs. Rigorous constitutive relationships in Abaqus allows to reliably model the behaviour of composite and reinforced concrete structures including concrete cracking, concrete crushing and reinforcement and steel decking yielding in addition to boundary conditions and steel-concrete interface bond behaviour.

A three-dimensional (3D) finite element model was developed to account for the material and geometric non-linearities in composite slabs. The interaction between the profiled steel decking (which act as reinforcement) and concrete and the presence of reinforcement provided to resist gravity loading or secondary effects like shrinkage and temperature was also considered.

Material Properties

The material of steel decking was modeled as an elastic-perfectly plastic material without any strain

hardening. The minimum yield stress and modulus of elasticity of the steel decking was considered as $f_{yd} = 500$ MPa and $E_{sd} = 200$ GPa, respectively. The reinforcing bars were also modelled as elastic-perfectly plastic material with $f_{yr} = 300$ MPa and $E_{sr} = 200$ GPa. The Poisson's ratio of $\nu_s = 0.3$ and the density of $\rho_s = 7750$ kg/m³ were selected for both steel decking and reinforcing bars.

The concrete damaged plasticity (CDP) model (Abaqus, 2011) was used to model the concrete slab. The damaged plasticity was assumed to characterise the uniaxial tensile and compressive response of concrete as shown in Fig. 2. When the tension stress reaches the failure stress σ_{t0} , failure stresses in concrete block are converted to replace micro cracking. Beyond the state of the failure stress in concrete, stress-strain response is presented by softening characteristic. For post-failure behaviour in tension, instead of a stress-strain curve, a stress-displacement curve is used to avoid any likely unreasonable mesh-sensitive results. Similarly, the compressive response in concrete is linear until reaching the initial yield stress σ_{c0} following stress hardening until the ultimate stress σ_{cu} and strain softening afterwards.

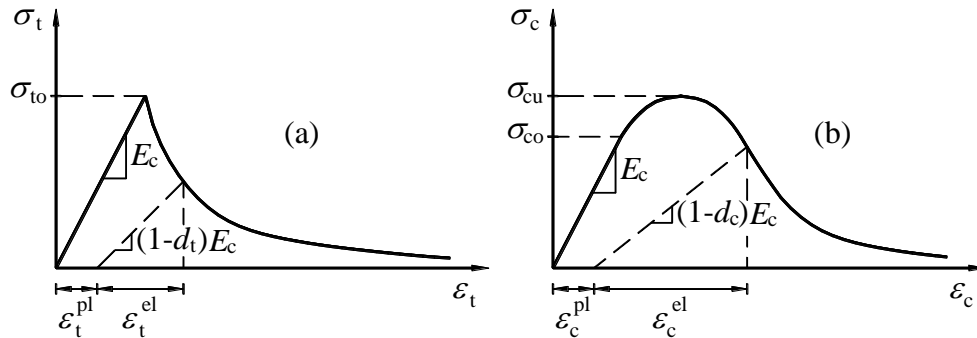


Figure 2. Stress-strain curves in concrete in tension including tension stiffening (a) and in compression with compression hardening (b).

The property values for CDP model were suggested by Kmiecik et al. (2011), NZS 3101 (2006) and Abaqus (2011) default values. The modulus of elasticity $E_{co} = 30$ GPa and maximum compression stress in uniaxial direction of $\sigma_{cu} = 32$ MPa were considered. The Poisson's ratio and the tension strength was considered to be $\nu_c = 0.2$ and $\sigma_{t0} = 3.4$ MPa, respectively. The coefficients of tensile and compressive stiffness degradation damage $d_t = d_c = 0$ were considered in the model. The density of concrete was $\rho_c = 2400$ kg/m³, and the reset of parameters were obtained from Abaqus default values.

Slab Geometry

The steel decking type Comflor 80 with 80 mm deep trough was selected in this study as shown in Fig. 3. The overall depth of the profile was 95 mm. The thickness of steel decking was $t_{sd} = 0.9$ mm. The overall slab thickness was variable in the study with $t = (130-150)$ mm as shown in Fig. 4. The overall slab length was 4.5 m in each direction. Nominal temperature and shrinkage resisting reinforcing bars were modelled as 10 mm diameter bars at 200 mm centres located on top of the decking profile (at a distance of 100 mm from the bottom of the slab) throughout the span of slab. In a 150 mm thick slab, this provided the reinforcement ratio of $\rho = 0.0035$ in cross section. The reinforcing bars were always placed with the same amount in two directions orthogonally.

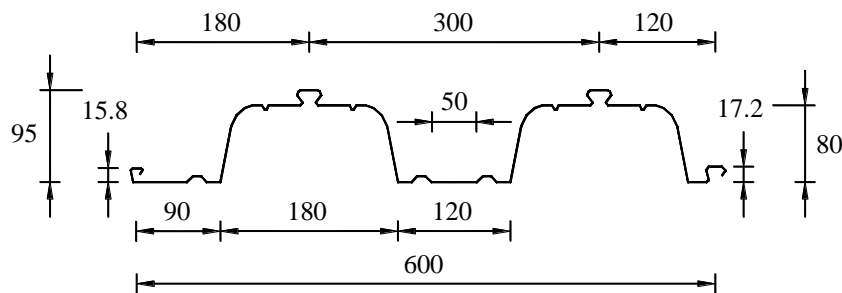


Figure 3. Dimensions of decking profile Comflor 80 (in mm).

The initial concrete thickness was selected as 150 mm. If all failure criteria were satisfied to ensure no failure occurred, the thickness of concrete slab was reduced until a failure occurred. Four different thicknesses namely as 150 mm, 140 mm, 135 mm and 130 mm were analysed, respectively.

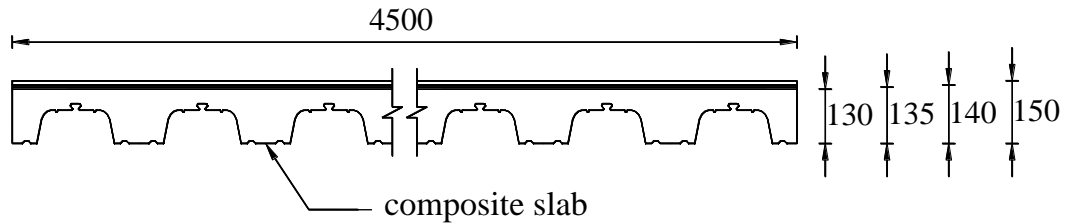


Figure 4. Simplified cross-section of slabs.

Modelling Elements

Three dimensional (3D) elements C3D8 and C3D20R were selected to model the steel decking and concrete slab. Gaussian quadrature is used in Abaqus for most elements to evaluate the material response at each integration point in each element. The C3D8 element is an 8-node linear brick element with 8 integration points whereas the C3D20R element is a 20-node quadratic element with 8 reduced integration points suitable for modelling the ultimate limit state analysis due to their high computational accuracy (Abaqus 2011). The size of the 3D elements was limited to 50 mm.

The steel rebar was modelled using truss element T3D2 having 2 nodes. The size of the T3D2 element was limited to 50 mm as well. The embedded element technique that specified an element or a group of elements was embedded in host region was used to model steel rebar. In this study, the embedded element and the host region were steel rebar and concrete slab, respectively. In this technique, the geometric relationships between the nodes of the steel rebar elements (embedded elements) and the concrete elements (host elements) is pursued and if the nodes of steel rebar element lies within a concrete element, the translational degree of freedom at those nodes is eliminated and the node becomes an embedded node. This means, the translational degrees of freedom of the steel rebar node are constrained to the interpolated values of the corresponding degree of freedom of the concrete elements.

Constraints and Boundary Conditions

The boundary condition was obtained from Comflor 80 construction manuals (by Steel & Tube Holdings (2008)). The minimum seating length to satisfy bearing requirements for end bearing and shared bearing on steel supporting beams was 50mm. In simple connection between the composite slab and the supporting beams, all three translation degrees of freedom per node in connecting nodes of steel decking were restrained as shown in Fig. 5a. To model the continuity of composite slabs over the supporting beams, all three translational degrees of freedom in concrete slabs were restrained in addition to all three translation degrees of freedom of steel decking as shown in Fig. 5b.

To model the inertia-induced forces in slabs, five models with different boundary conditions were generated and analysed as shown in Fig. 6. Model 1 represents a composite slab that is simply-supported on top of four supporting beams. Model 5 represents an internal panel of a composite floor in which both steel decking and concrete slab are continuous over supporting beams whereas Model 2 represents the corner panel in the same floor. Models 3 and 4 represent the edge panels depending on the orientation of steel decking ribs. Two models were also generated and analysed to evaluate the effects of transfer forces in composite slabs as shown in Fig. 7. The fixed support in Models 6 and 7 in fact may represent a rigid shear wall to which the transfer/shear forces are transmitted from the adjacent frame. Although not strictly correct, it was assumed that the perfect interface connection was available between surface of concrete slab and steel decking.

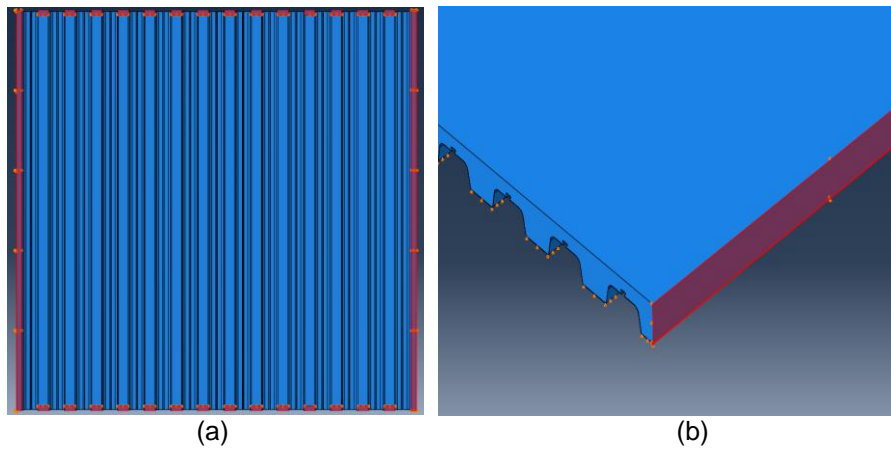


Figure 5. Simple connection between composite slab and supporting beams (a) concrete slab continuity in a fixed support model (b).

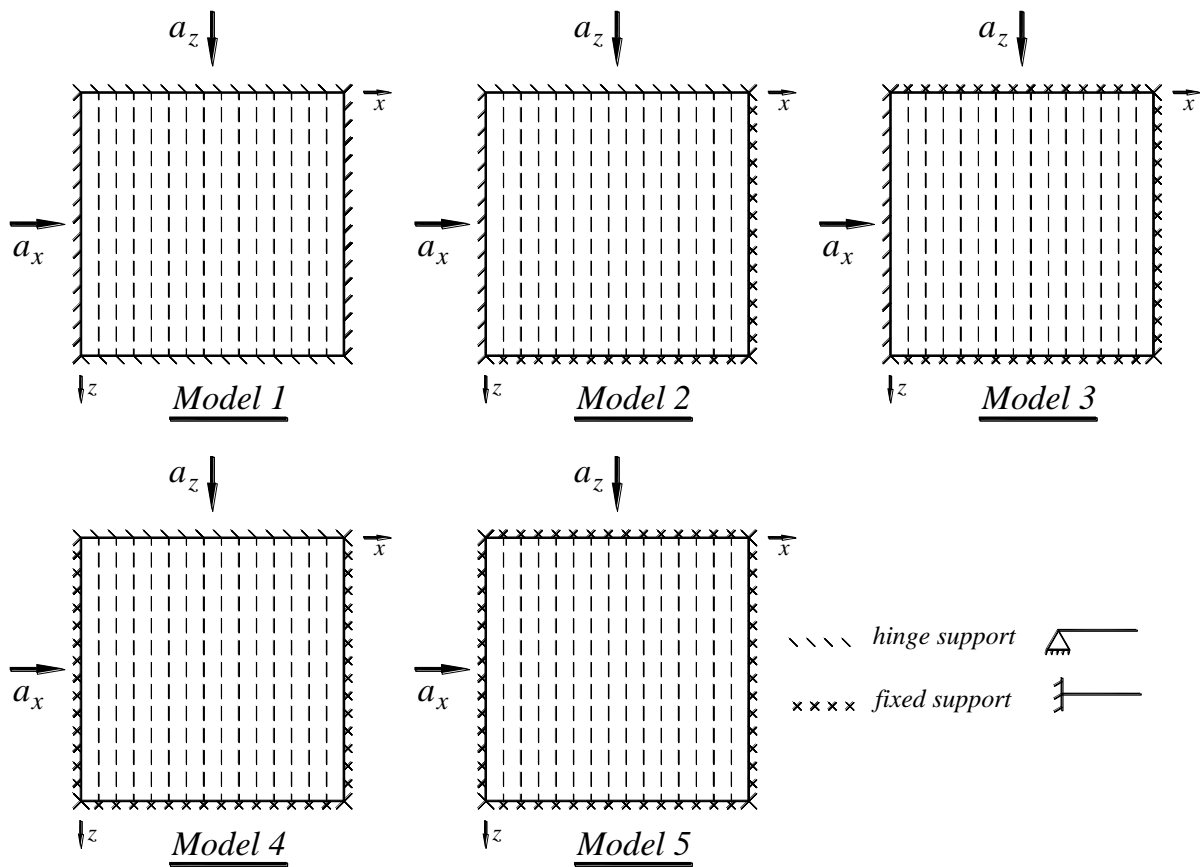


Figure 6. Different models analysed for inertia-induced forces.

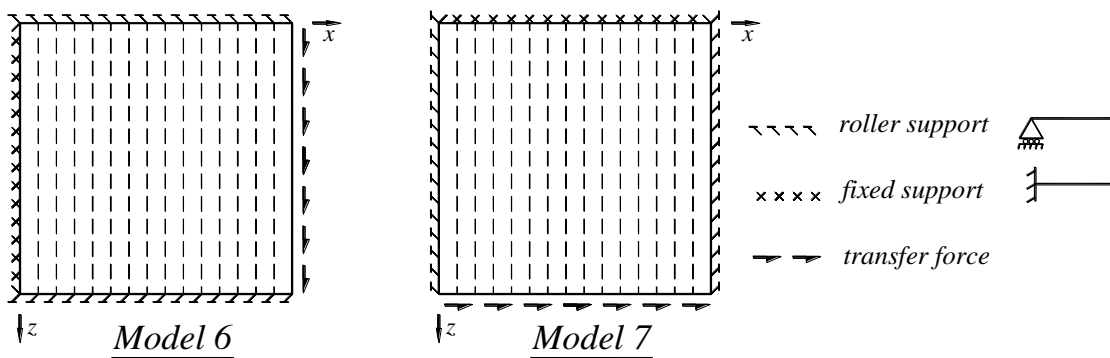


Figure 7. Different models analysed for transfer forces effects.

Loadings

The gravity loads including self-weight of the slabs and superimposed live load of 3 kPa was applied on the top surface of composite slabs.

The maximum design acceleration in floor was obtained from ASCE 7 (2002). In a diaphragm, the design force for each floor is calculated as:

$$F_{pj} = \frac{\sum_{i=j}^n F_i}{\sum_{i=j}^n w_i} w_{pj} \quad (1)$$

where F_{pj} is the diaphragm design force at level j ; F_i is the design seismic force applied to the i -th level; w_i is the seismic weight of the i -th level and w_{pj} is the seismic weight of the diaphragm at level j . This design force has an upper bound value of $0.4S_{DC}/w_{pj}$ where S_{DC} is the design spectral response acceleration at short periods and I is the occupancy importance factor, respectively. The design spectral response acceleration at short periods S_{DC} is calculated as:

$$S_{DC} = (2S_{MS}) / 3 \quad (2)$$

$$S_{MS} = F_a S_s \leq 1.6g \quad (3)$$

where the parameter F_a is acceleration-based site coefficient and its value depends on the value of S_s and site location and S_s is the mapped maximum considered earthquake spectral response acceleration at short period that ranges between $0.4g$ to $1.5g$. The occupancy importance factor depends on the nature of occupancy and assuming Category III (commercial buildings) the occupancy importance factor was $I = 1.25$. Therefore, with the maximum value of $F_a S_s = 1.6g$ the maximum diaphragm design force was $F_{pj} = 0.55w_{pj}$ indicating that the maximum design acceleration was $a_{pj} = 0.55g$. In Models 1-5, this acceleration was applied on the mass centroid of composite slabs by using gravitational acceleration as either $a_x = 0.55g$ or $a_z = 0.55g$ at a time. Similarly, with selected live load magnitude of $Q = 3$ kPa and earthquake-imposed combination factor for live load as $\Psi_E = 0.3$ in accordance with NZS 1170.5:2004, the earthquake-induced forces due to live load was obtained as $F = 0.55 \times 0.3 \times 3 = 0.5$ kPa and was applied on the top surface of slabs in either x or z direction, respectively.

In Models 6 and 7, monotonically increasing forces were exerted on one side of slab and the corresponding deformation was monitored until a target deformation was reached and total force versus deformation was plotted for all steps.

Analysis

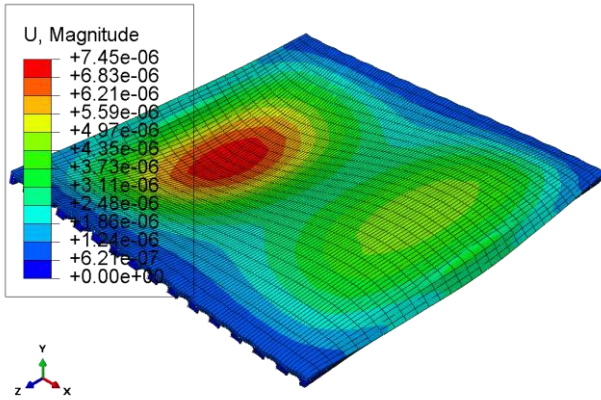
In static analysis for inertia-induced forces, ultimate gravity load in y direction, inertia acceleration in either x or z direction and combination of these two load conditions were applied to the composite slabs. Tresca and Bresler-Pister yield criteria (Labbane et al. 1993) were used to verify if steel and concrete strength satisfied all analysis conditions. If all limit states were satisfied in all models, the slab thickness was then reduced until a type of failure occurred. In total, four different slab thicknesses namely as 150 mm, 140 mm, 135 mm and 130 mm were analysed.

Each model was analysed with and without steel rebar to differentiate the effects of inclusion of reinforcement in slab. Due to the different slab properties in x and z directions, all accelerations were applied in either x or z direction, respectively. In limit state analysis for transfer forces effects, the in-plane shear strength of slabs was determined in a displacement control manner. Similarly, four slab thicknesses with and without steel rebar were analysed.

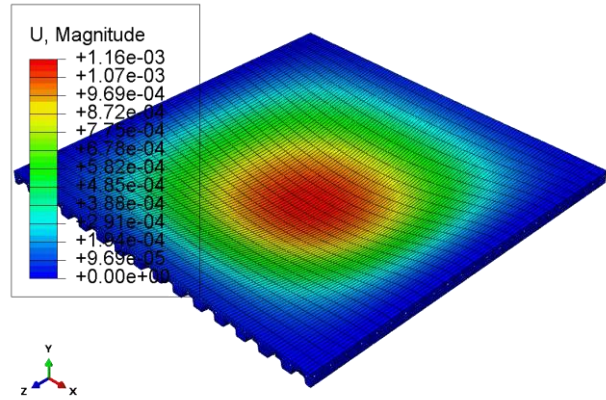
Results and Discussion

The resultant deformation is defined here as $U = (U_x^2 + U_y^2 + U_z^2)^{0.5}$ where U_x , U_y , U_z are the deformations in x and y and z directions, respectively and the gravity load is applied in y direction. When inertia-induced forces were applied to the slabs, the resultant deformations were negligible compared to the deformations due to gravity loading meaning the total deformation was mainly as a result of gravity loads (i.e. the slab self-weight and live load), and hence the maximum deformation occurred at centre of slab. This can be seen in Fig. 8 which compares the deformation magnitudes in 150 mm thick slab Model 1 when only in-plane inertia accelerations were applied in x direction and when both the in-plane inertia accelerations in x direction and

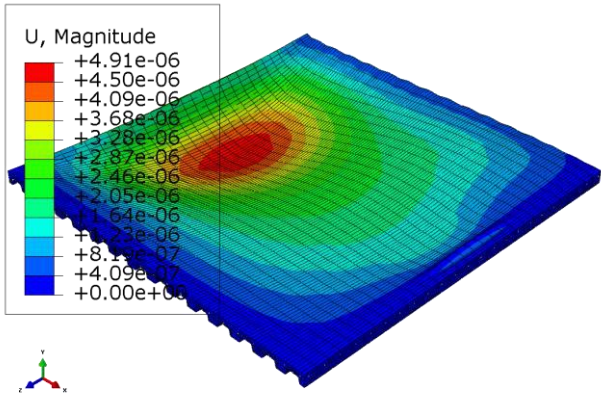
gravity loads were applied. For the applied in-plane inertia accelerations on the slab, double curvature in the slab occurred with rotation of free concrete faces. However, the maximum resultant deformation of the slab was quite negligible and was about 7.45×10^{-3} mm whereas for the combination of in-plane inertia accelerations and gravity loads the maximum deformation of the slab occurred in centre of slab and was 1.16 mm. Similar results were found as a result of analysing Models 2-5 as shown in Fig. 8. It should be noted that due to lesser stiffness and strength of slabs in x direction, only the deformations due to in-plane inertia accelerations in x direction have been presented. As expected, the deformations in slabs with steel rebar and slabs without steel rebar were quite similar.



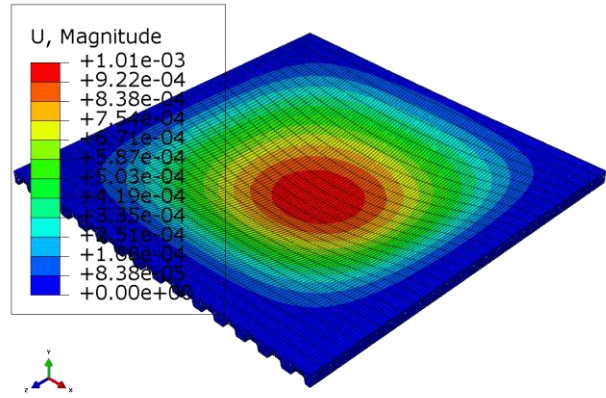
(a) Model 1



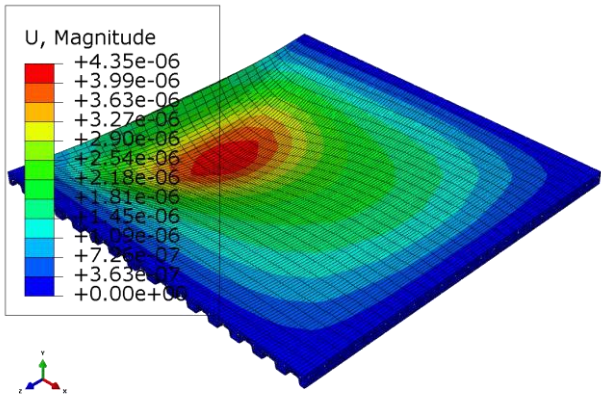
(b) Model 1



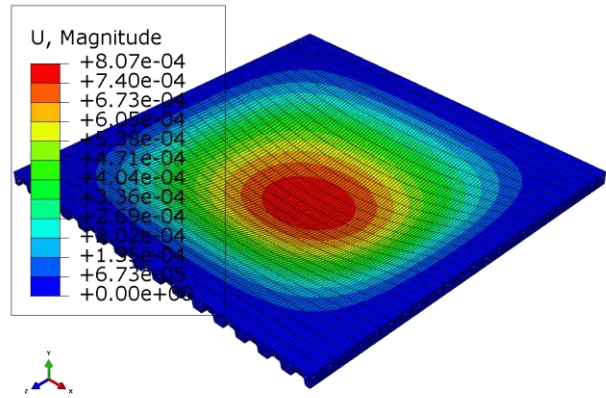
(a) Model 2



(b) Model 2



(a) Model 3



(b) Model 3

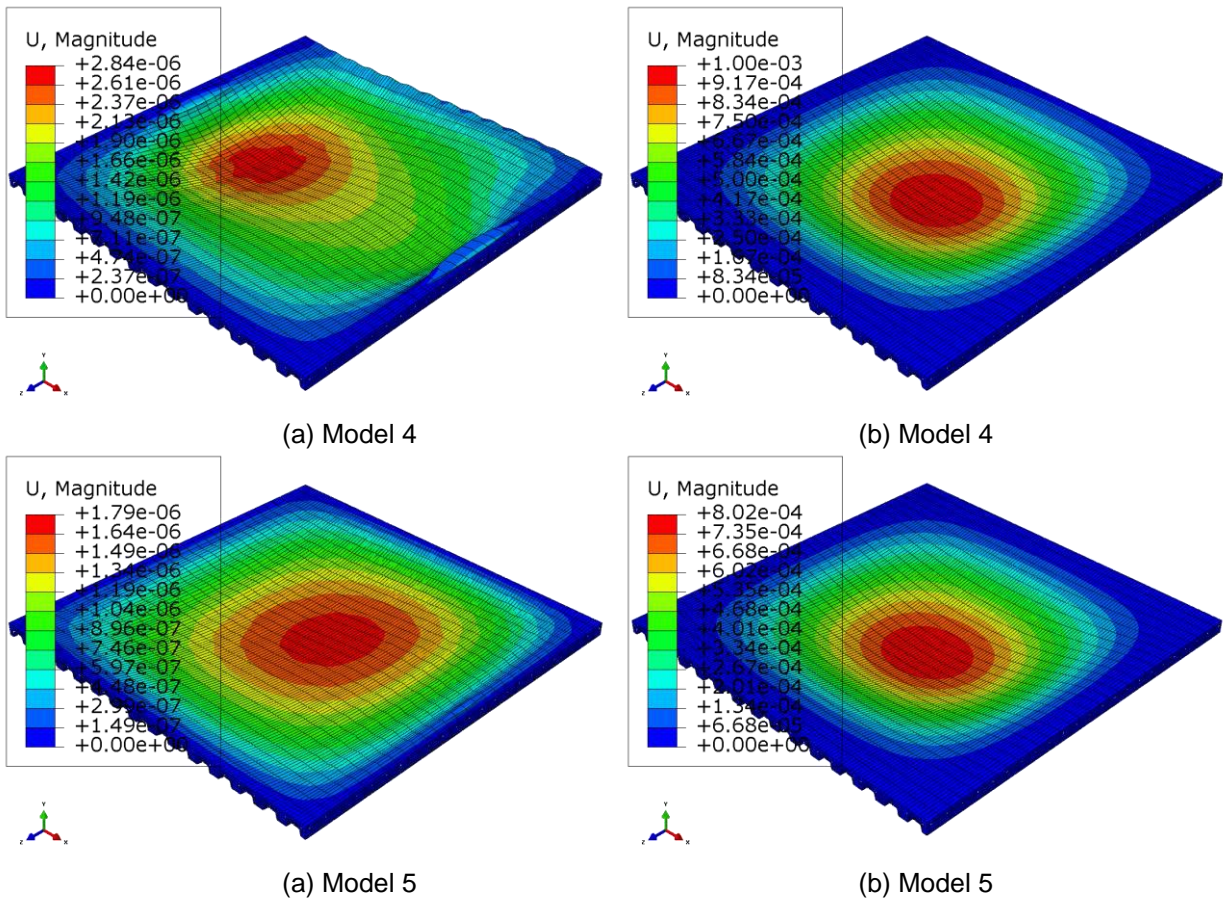


Figure 8. Deformation (in m) of 150 mm thick slab with steel rebar in Models 1-5 under in-plane inertia-induced forces in x direction (a) and combination of in-plane inertia-induced forces in x direction and gravity loads (b).

In multiple slab thickness analyses, when the thickness of unreinforced slab was reduced to 130 mm in Model 5, tension cracking occurred on the top surface of the thinnest part of concrete slab as presented in Fig. 9. When the steel rebar was modelled in the slab, since it was placed on top of the steel decking, the resultant stress in steel rebar was initially compressive. The rebar was ineffective to control tension cracking and retain the cross-section strength, and hence sudden failure occurred and negligible load at this stage was resisted by cracked cross-section and bare steel decking profile.

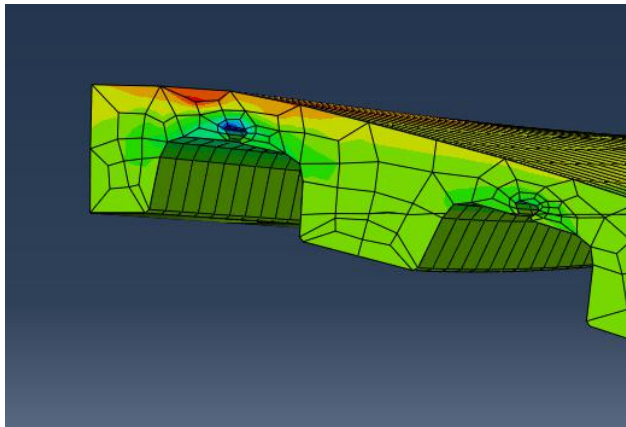


Figure 9. Cross-sectional view of tension failure in a 130 mm thick unreinforced slab in Model 5.

The variation of total applied load versus slab deformation in Models 6 and 7 is shown in Figs. 10 and 11. Obviously, in all cases the shear strength of slabs was increased when the slab thickness increased or steel rebar included. The shear strength in Model 6 in a 150 mm thick unreinforced slab was 258 kN and when reinforcement was included, the strength increased significantly by a factor of 1.82 to 470 kN. Similar results were obtained in other slabs in Model 6. In unreinforced slabs in Model 6, after deformation of 4 mm, the

shear strength remained constant in the range of 140 kN to 170 kN. This means that after concrete cracking in tension, all the strength of slabs was due to bending the steel decking about its neutral axis and the capacity of steel decking to carry transfer forces was about (140-170) kN. However, when reinforcement included, the shear strength increased considerably as a result of resistance of steel rebars against tensile stresses. In unreinforced slabs, the peak load capacity was achieved when the slabs deformed about 0.75 mm. This is actually when the concrete firstly cracked in tension and the load was resisted by steel decking only. However, in reinforced slabs the presence of steel rebars increased both strength and ductility as the peak load was achieved at deformation of about (2-3) mm.

The behaviour of slabs in Model 7 followed quite a different pattern than that in Model 6 which apparently was as a result of different orientation of steel decking ribs together with slab deep-beam action when transferring the loads. In a 150 mm thick unreinforced slab in Model 7, the ultimate shear strength was 1415 kN and when the steel rebar was included, the strength increased by a factor of 1.11 to 1565 kN. The ultimate strength was achieved when unreinforced and reinforced slabs deformed about 30 mm.

Apparently the slabs were considerably weaker to transfer shear forces if the applied in-plane transfer forces were parallel to steel decking ribs (i.e Model 6) or the slabs were unreinforced. This is because in Model 6, the transfer forces are mainly resisted by slab clear thickness above the steel decking whereas in Model 7, the whole cross-section is effective in carrying the transfer forces. In addition, in Model 6 the steel decking is considerably more flexible than that in Model 7 where the steel decking bends about its strong axis. This highlights the key role played by detailing in design of a composite slab to carry in-plane transfer forces by properly considering the orientation of steel decking and placing sufficient reinforcement. Additional attention should be paid to other issues when detailing a composite slab such as anchorage of steel rebars to reach the yield stress.

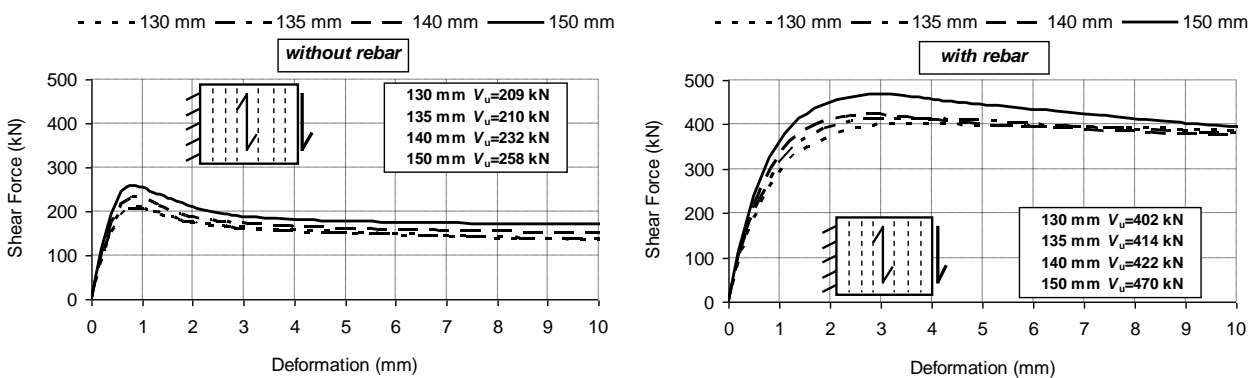


Figure 10. Total shear force vs. slab deformation in Model 6.

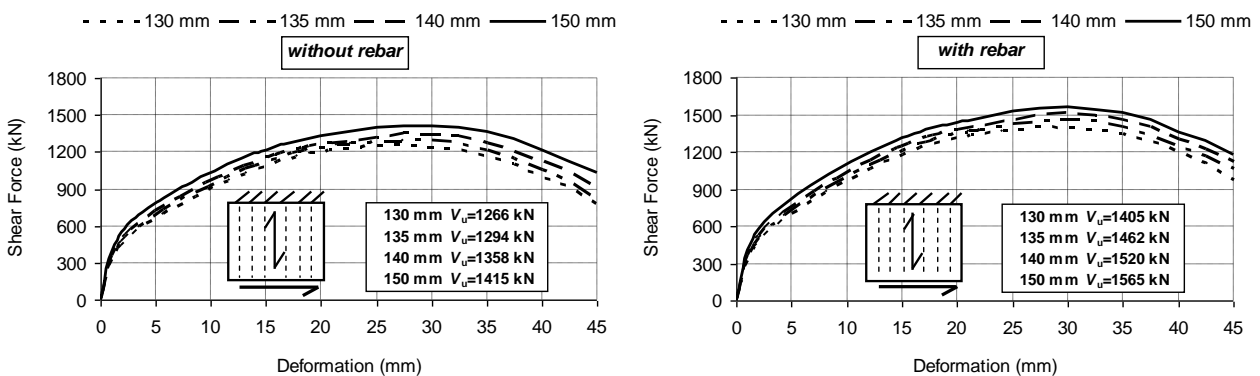


Figure 11. Total shear force vs. slab deformation in Model 7.

Conclusions

The behaviour of composite concrete slabs with steel decking for a certain geometry and steel decking type has been investigated in this paper using the finite element method. In a 4.5 m square-in-plan slab with a 95 mm deep steel decking profile and for a selected loading condition, in multiple numerical analyses it was found that:

- 1) The effects of in-plane forces on out-of-plane deformations were negligible and the total deformation was mainly as a result of gravity loads.
- 2) For a 150 mm thick slab with reinforcement ratio of 0.0035, when the load was applied parallel to steel decking ribs, the strength of slab to carry in-plane transfer forces was 82% greater than that in unreinforced slab (470 kN vs. 258 kN).
- 3) However, in the same slab when the load was applied perpendicular to steel decking ribs, the strength of slab was only 11% greater when reinforcement included compared to that in unreinforced slab (1565 kN vs. 1415 kN).
- 4) The slab strength when the in-plane transfer forces were applied perpendicular to the steel decking ribs orientation was 3.33 times of that in the parallel direction for one case (1565 kN vs. 470 kN).
- 5) For slab thickness less than 135 mm (i.e. 40 mm concrete slab above the steel decking) tensile failure occurred at the thinnest part of concrete slab and placing rebar on top of steel decking was ineffective to prevent the failure.

Acknowledgments

The work reported herein has been undertaken with the financial support of The University of Canterbury and Earthquake Commission (EQC). This support is gratefully acknowledged.

References

- Abaqus, 2011. *Abaqus Analysis User's Manual*, Version 6.11. Dassault Systems.
- ASCE 7 (SEI/ASCE 7:2002), *Minimum Design Loads for Buildings and other Structures*, 2nd Edition, American Society of Civil Engineers, Virginia, US.
- Chaudhari, T., MacRae, G., Bull, D., Chase, G., Hobbs, M., Clifton, C., Hicks, S., 2014. Composite Slab Effects on Beam-Column Subassemblies: Further Development, *Paper 06, New Zealand Society for Earthquake Engineering Annual Conference (NZSEE)*, Auckland, New Zealand
- Kmiecik, P., and Kaminski, M., 2011. Modelling of Reinforced Concrete Structures and Composite Structures with Concrete Strength Degradation Taken into Consideration, *Archives of Civil and Mechanical Engineering*, 11(3), 623-636.
- Labbane, M., Saha, N. K., & Ting, E. C., 1993. Yield Criterion and Loading Function for Concrete Plasticity, *International Journal of Solids and Structures*, 30(9), 1269-1288.
- New Zealand Standard (NZS 1170.5:2004), *Structural Design Actions-Part 5: Earthquake Actions*, Standards New Zealand, Wellington.
- New Zealand Standard (NZS 3101:2006), *Concrete Structures Standard*, Standards New Zealand, Wellington.
- Steel & Tube Holdings Ltd., 2008, *ComFlor 80 Product Guide*, Auckland, New Zealand.